

<sup>1</sup> Sharanya S<sup>2</sup> Sabanayakar S<sup>3</sup> Ashwin G<sup>4</sup> Ajitha U

## Enhancing ECG Monitoring with Wearable Nanosensor



**Abstract:** - Electrocardiography (ECG) is an essential tool for monitoring heart activity, but conventional electrodes often face limitations such as discomfort, signal degradation, and high contact impedance. This project focuses on developing a wearable nanosensor-based electrode for ECG tracing, enhancing signal acquisition accuracy and user comfort. By integrating nanosensors into the electrode, the system effectively captures bioelectrical signals with minimal interference and improved conductivity. The captured ECG signal involved in signal conditioning circuit comprising amplification and filtering stages to enhance signal clarity. The conditioned signal is displayed in real-time on a user interface, allowing for continuous monitoring and analysis. This wearable nanosensor-based system provides improved flexibility, biocompatibility, and accuracy compared to traditional ECG electrodes. The proposed technology is highly suitable for remote health monitoring, wearable medical devices, and real-time cardiac diagnostics. By leveraging nanotechnology, this project aims to advance ECG monitoring with enhanced portability, reliability, and ease of use, contributing to the development of next-generation personalized healthcare solutions.

**Keywords:** Nanosensor, Signal Conditioning, Biocompatibility.

### I. INTRODUCTION

To prevent sudden heart attack and fatal complications in severe stages, early diagnosis is an utmost importance. Electrocardiogram (ECG) is one, simple diagnostic method. ECG devices record electrical signal from cardiac muscle to analyze the abnormality present in the heart [1]. This novel ECG nano-sensor utilizes piezoelectric effect for biometric data collection, utilizing low power and efficient communication interfaces for patient monitoring and data gathering [2]. The signal conditioning circuit converts the acquired raw signal to normal ECG signal [3]. ECG signals are typically very small (in the millivolt range) and can be affected by various sources of noise. To avoid loading the signal source, the amplifier should have a high input impedance and sufficient gain to bring the signal to a measurable level [4]. ECG signals are prone to interference with noise of (50/60 Hz), muscle artifacts, and other environmental noise. Proper shielding, filtering, and amplification techniques are crucial to minimizing these interferences [5,6]. ECG signals frequently utilize instrumentation amplifiers due to their high input impedance, high common-mode rejection ratio, and effective differential signal amplification [7,8]. We use both high-pass and low-pass filters in ECG signal processing to remove noise and enhance signal quality [9]. High-pass filter with a cut-off frequency around 0.5–1 Hz to eliminate baseline wander and low-frequency noise [10]. Typically, prefer an active high-pass filter because it amplifies weak ECG signals, resulting in minimal signal distortion and improved performance. The low-pass filters with a cutoff near 100 Hz are utilized to eliminate high-frequency noise [11].

The ECG signal processing employs filters to capture essential components like P wave, QRS complex, and T wave, and a notch filter to eliminate power line interference at 50 Hz or 60 Hz [12,13]. It selectively filters out this narrow frequency band while preserving other important components of the ECG signal. An VP.in (Visual Programming Interface) is used to connect to a signal conditioning circuit and look at the R peak of the ECG data. Analyzing the peak of the ECG signal from the filtered circuit can detect intricate changes in bioelectrical signals, improving early diagnosis of heart conditions. The acquired ECG signal (current) from fabricated nano sensor has high accuracy and the electrodes are re-usable [14,15,16,17]. The traditional ECG system places gel-based electrodes (Ag/AgCl) on the chest and limbs. The system requires a clinical setup and wiring for accurate readings. While it provides high signal quality, it is susceptible to motion artifacts, electrode displacement, and skin irritation due to the use of conductive gels. In contrast, the wearable nanosensor gel includes zinc oxide, polyvinylidene fluoride, and carbon black that offer a non-invasive, flexible, and portable alternative. It uses dry-contact nanosensors that make it more sensitive and cut down on noise by about 30 db. Nanosensor-based systems optimize for low power consumption, making them ideal for continuous monitoring, unlike traditional ECGs that consume more power due to complex circuitry.

<sup>1</sup> Department of Electronics and Instrumentation Engineering, SRM Institute of Science and Technology, Kattankulathur, Chennai, TamilNadu, India. sharanyas@srmist.edu.in

<sup>2</sup> Department of Electronics and Instrumentation Engineering, SRM Institute of Science and Technology, Kattankulathur, Chennai, Tamil Nadu, India. ss1038@srmist.edu.in

<sup>3</sup> Department of Electronics and Instrumentation Engineering, SRM Institute of Science and Technology, Kattankulathur, Chennai, Tamil Nadu, India. ag9993@srmist.edu.in

<sup>4</sup> Department of Electronics and Instrumentation Engineering, SRM Institute of Science and Technology, Kattankulathur, Chennai, Tamil Nadu, India. au3935@srmist.edu.in

Copyright © JES 2024 on-line: journal.esrgroups.org

## II. SYNTHESIS AND FABRICATION OF NANOSENSOR

Synthesis and fabrication of nanosensors involve the preparation of nanomaterials, such as ZnO and graphene, through chemical processes to achieve desired properties. The fabricated nanosensors are then integrated into functional devices for applications in sensing, electronics, and biomedical fields. The synthesis of zinc oxide (ZnO) begins with the preparation of zinc acetate and oxalic acid solutions. A 0.1M solution of zinc acetate dihydrate is dissolved in 100 mL of distilled water, while a 0.15M solution of oxalic acid is prepared separately. These solutions are mixed and stirred continuously for three hours at room temperature, leading to the precipitation of zinc oxalate. The precipitate is then filtered, washed with distilled water and ethanol to remove impurities, and dried at room temperature. The dried zinc oxalate undergoes annealing at 200°C for four hours, resulting in the decomposition of zinc oxalate into ZnO nanoparticles. To synthesize graphene, coconut shells are selected as the carbon source, burned to remove non-carbon elements, and ground into a fine powder. The powder undergoes carbonization at 800°C for two hours, transforming the amorphous carbon into structured graphitic layers suitable for graphene production.

For the ZnO/graphene composite, 100 mg of ZnO and 50 mg of graphene are mixed in a solvent such as water or ethanol to achieve uniform dispersion. Sonication for 20 minutes ensures the proper interaction of ZnO with graphene sheets, breaking up aggregates for a homogeneous mixture. After sonication, the composite is filtered, dried, and collected as a solid powder, ready for applications in sensors, energy storage, and optoelectronic devices. The final electrode formulation consists of ZnO, polyvinylidene fluoride (PVDF) as a binder, and carbon black for enhanced electrical conductivity. The resulting slurry is coated onto the electrode surface, ensuring effective integration of materials for improved performance. The Figure 1 shows the solution and Figure 2 shows the solution coated onto the electrode.



Figure 1: ZnO/Graphene solution



Figure 2: Solution coated onto the electrode

## III. ROLE OF NANOSENSOR

The piezoelectric sensor attached to the electrode in the powdered form in addition to carbon and polymer particles which improve the conductivity. This sensor detects the mechanical vibrations generated by heart muscle contractions (depolarization) and relaxations (re-polarization). Generates a small electrical signal proportional to the mechanical activity. The electrode is attached to right and left arm of the hand as well as in left leg. The Piezoelectric materials generate a small electrical signal when subjected to mechanical stress or pressure. The current output is proportional to the force applied. sensor is subjected to 3 leads to acquire an electrical signal. The acquired electrical signal undergoes a signal conditioning circuit to amplify, followed by the removal of noise using a filter circuit. A piezoelectric sensor is created using zinc oxide, polyvinylidene fluoride, and carbon black particles combined in an 8:1:1 ratio coated with the electrodes, enabling accurate signal acquisition. The following are the characteristics of nanosensor:

- \* **High Sensitivity Detection:** Nanosensors can detect weak bioelectrical signals from the heart with higher precision compared to conventional electrodes to the range of  $10^{-9}$ .

- \* **Enhanced Signal Quality:** They improve ECG signal clarity by reducing baseline drift, motion artifacts, and electrical noise.

- \* **Improved Conductivity:** Materials like ZnO, PVDF, and carbon black enhance electrical conductivity, ensuring efficient signal transmission.

- \* **Real-Time Data Processing:** They facilitate continuous, real-time ECG monitoring with wireless integration for remote healthcare applications.
- \* **Miniaturization and Wearability:** Due to their small size and flexibility, nanosensors enable compact, lightweight, and wearable ECG devices for continuous monitoring.

IV. BLOCK DIAGRAM

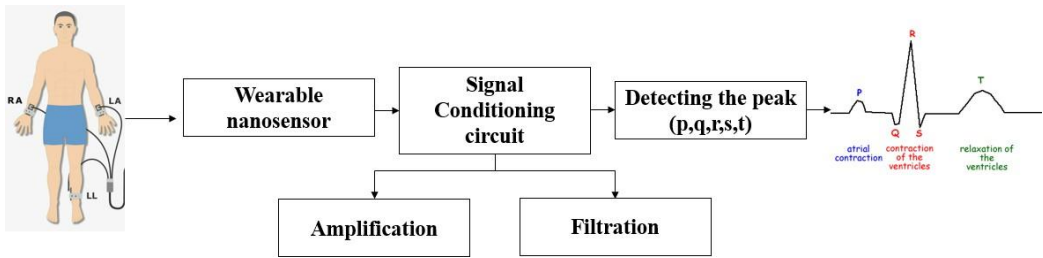


Figure 3: Block diagram of the proposed model

V. SIGNAL CONDITIONING CIRCUIT

I. AMPLIFICATION:

The LM741-based instrumentation amplifier has three bioelectrodes in total, two of which function as differential potential terminals and supply the ECG vector to the terminals with a CMRR value of 96 dB at a slew rate of 0.5V/ $\mu$ s. The INA is a crucial element in ECG signal amplification, necessitating a high Common-Mode Rejection Ratio (CMRR) to effectively reject noise and amplify the differential ECG signal. It also amplifies the potential difference between two points, maintains a high input impedance, introduces minimal noise to preserve signal quality, and maintains a low offset voltage and minimal drift to maintain steady baseline and avoid artifacts. The circuit diagram is being designed in LTSpice and simulated using an AC sweep from 1 to 1kHz, the final op amp design produced a gain of 1000, which is nearly identical to the desired gain of 1008, thus shown in the Figure 4 and Figure 5.

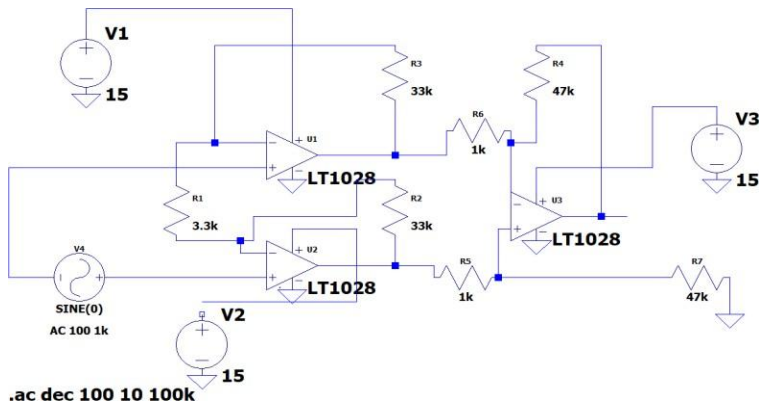


Figure 4: Circuit Diagram of instrumentation amplifier

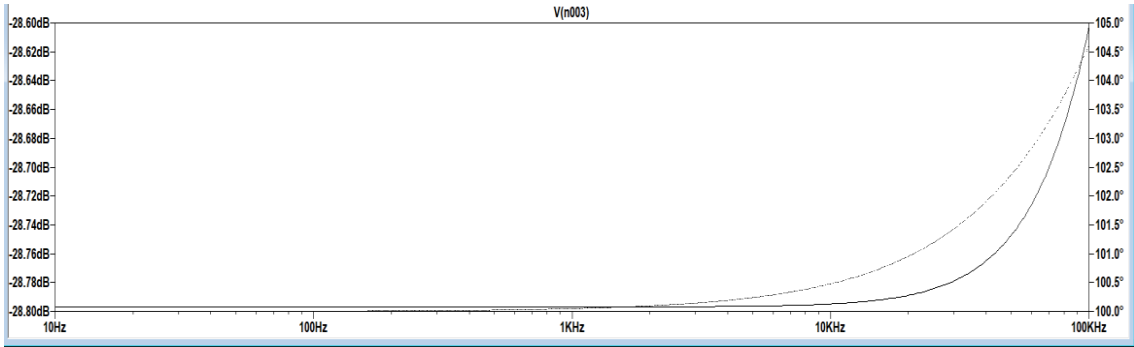


Figure 5 : Simulated Output for Instrumentation amplifier

## A) Calculation: Instrumentation Amplifier:

By using:  $R_1 = 3.3k$  ohms,  $R_2 = 33k$  ohms,  $R_3 = 1k$  ohms,  $R_4 = 48$  ohms.

$$\begin{aligned}
 A_v &= \frac{-R_4}{R_3} \left( 1 + \frac{R_2}{R_1} \right) \\
 &= \frac{-48}{1k} \left( 1 + \frac{33k}{3.3k} \right) \\
 &= -1008
 \end{aligned} \tag{1}$$

Where,  $A_v$  = Gain of the instrumentation amplifier, From the graph we found  $\text{Gain} = 10^{\frac{60}{20}} = 1000$  which is sufficiently close to our intended gain of 1008. The equation (1) shows the gain value of instrumentation amplifier.

## II. FILTRATION:

## A) High Pass Filter:

The filter eliminates low-frequency noise, such as baseline wander approximately 25 db. The cut-off frequency is typically around 0.5 Hz, ensuring that essential ECG components, such as the P-wave, remain unaffected. By setting the cutoff at 0.5 Hz, this can attenuate low-frequency noise while retaining essential ECG features, such as slow heart rate signals (e.g., bradycardia). When the desired cutoff is too high ( $>0.5$  Hz) can distort ST-segment variations, which are essential for identifying ischemia or myocardial infarctions. Hence the desired cut off is set at 0.5 Hz. The circuit diagram and simulated output is shown in the Figure 6 and Figure 7.

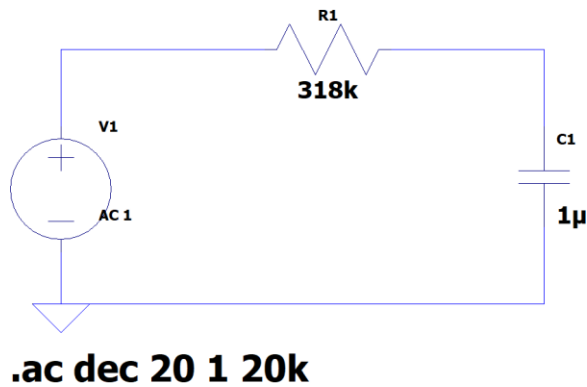


Figure 6: Circuit diagram of High pass filter

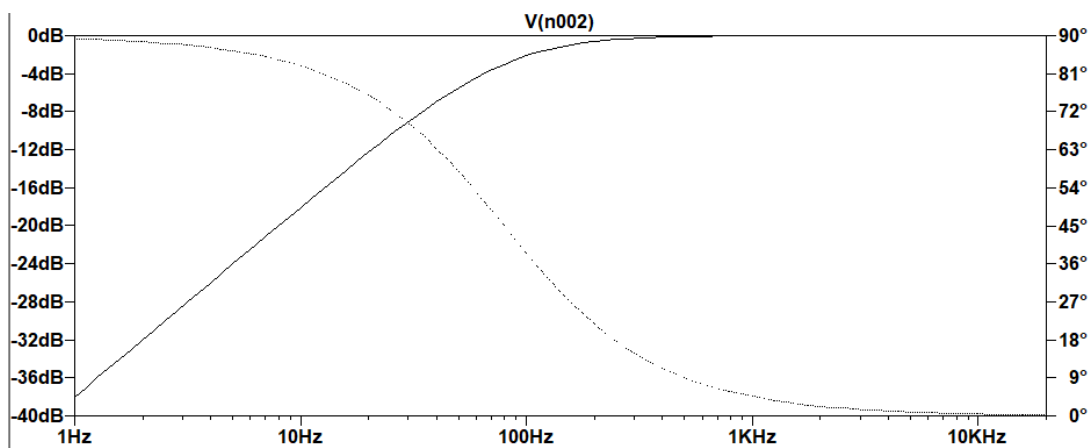


Figure 7: Simulated output for High pass filter

## B) Calculation for high pass filter:

By using:  $f = 0.5$  Hz, and  $C = 1$  uF

$$\begin{aligned}
 R &= \frac{1}{2 \times \pi \times 0.5 \times 1} \\
 &= 318 \text{ k Ohm}
 \end{aligned} \tag{2}$$

The resistor value of high pass filter is given in the equation (2).

### C) Low Pass Filter:

It helps remove high-frequency noise, such as muscle artifacts and electrical interference from the environment. Desired cut-off frequency: 100 Hz. The filtering process gets rid of unwanted high-frequency signals by 30 dB while keeping the integrity of the QRS complex and T-wave. Most of the energy in ECG signals is found below 100 Hz, and important patterns like the QRS complex, P-wave, and T-wave usually occur between 0.05 Hz and 100 Hz. The Muscle movements and external electrical sources mostly produce noise at frequencies above 100 Hz. By Setting the limit at 100 Hz helps eliminate muscle noise but keeps the QRS complex clear, which has frequencies up to 40–50 Hz. If the cutoff is too low (below 100 Hz), it could affect the QRS complex, which may result in incorrect heart rate and rhythm measurements. A low-pass filter was created to remove data above the interest threshold, including ECG signals, using LTSpice with an AC sweep and 0.1 V sine wave input. The circuit diagram and simulated output is shown in the Figure 8 and Figure 9.

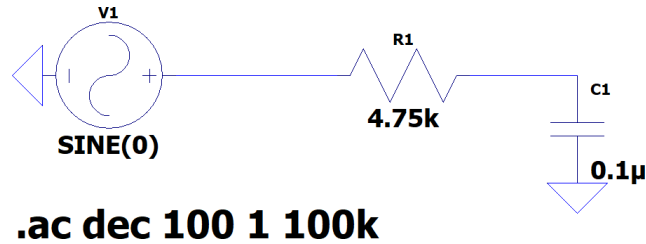


Figure 8: Circuit diagram of Low pass filter

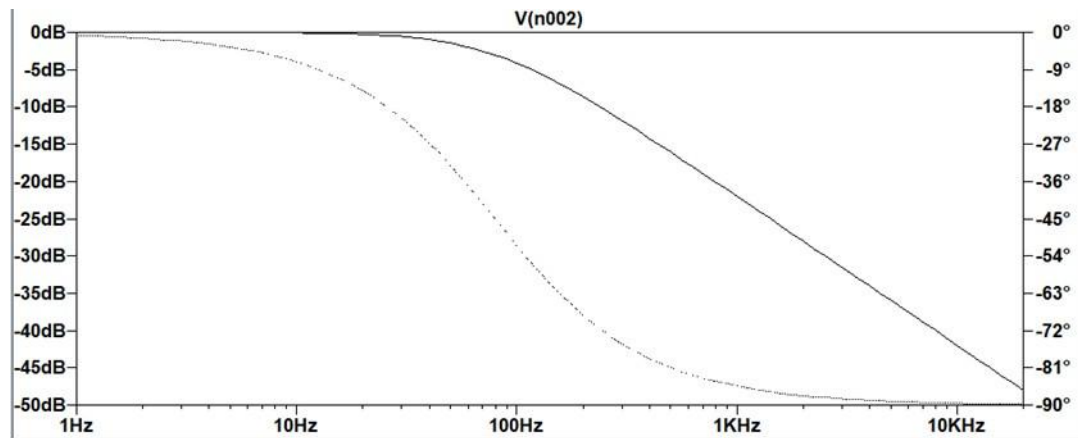


Figure 9: Simulated output of Low pass filter

### D) Calculation for low pass filter

The capacitor value is given by,

$$C=0.1 \mu\text{F}$$

$$R = \frac{1}{2 \times \pi \times 0.1 \times (10^{-6}) \times 335 \text{ Hz}} \quad (3)$$

$$= 4.75 \text{ k Ohm}$$

The resistor value of low pass filter is given in the equation (3).

### E) Notch Filter:

The primary use of a notch filter in ECG circuits is to remove the mains hum (power line interference) that contaminates the signal. It eliminates this specific frequency (50 Hz) without distorting the ECG waveform. The filter achieves a 40 dB reduction in power line noise. A notch filter circuit removes a specific frequency component from a signal (50/60Hz), removing power line interference. It creates a narrow band-stop effect using reactive components, attenuating the specified frequency while maintaining other frequencies, enhancing output quality. The filter's gain is one without amplifying characteristics. With an input voltage of 1 V, simulation on LTSpice efficiently reduces 60 Hz noise to 0.01 V, therefore yielding a gain of 1. The resistor and capacitor values are assigned based on the gain value and the output is verified using LTSpice software. The circuit diagram and output are shown in the Figure 10 and Figure 11.

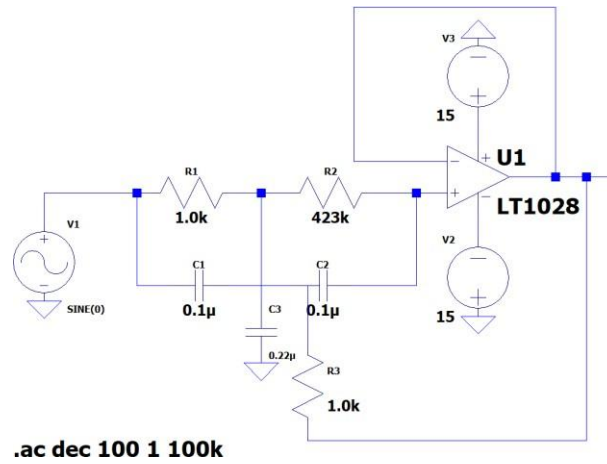


Figure 10: Circuit diagram of Notch filter

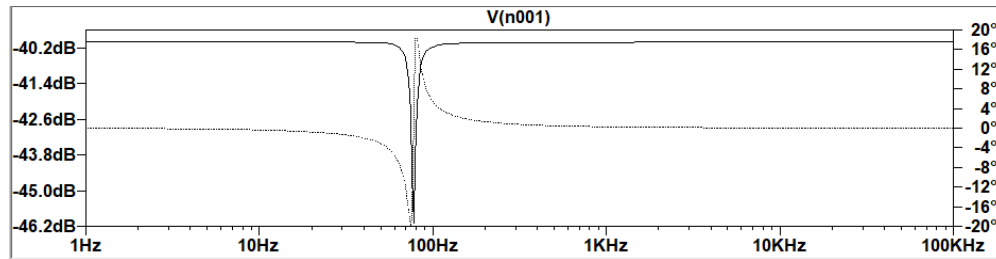


Figure 11: Simulated output of Notch filter

F) Calculation for notch filter:

The capacitor and Q factor value are given by,

$$C = 0.1 \mu\text{F}$$

$$2C = 0.2 \mu\text{F}, Q = 8$$

$$R_1 = \frac{1}{2 \times Q \times 2 \times \pi \times f \times c} \quad (4)$$

$$= \frac{1}{2 \times 8 \times 2 \times \pi \times 60 \times 1 \times 10^{-6}}$$

$$= 1.66 \text{ k Ohm}$$

$$R_2 = \frac{20Q}{2 \times \pi \times f \times c} \quad (5)$$

$$= \frac{20 \times 8}{2 \times \pi \times 60 \times 1 \times 10^{-6}}$$

$$= 424 \text{ k Ohm}$$

$$R = \frac{R_1 \times R_2}{R_1 + R_2} \quad (6)$$

$$= \frac{1.8 \text{ k} \times 423 \text{ k}}{1.8 \text{ k} + 423 \text{ k}}$$

$$= 1.79 \text{ k Ohm}$$

The signal reaches its lowest voltage at approximately 60 Hz. Because the input voltage is 1V, the filter successfully reduces 60 Hz noise to an undetectable level of 0.01V while delivering a gain of 1. The resistor value is identified in equation (4), (5), (6).

## VI. USER INTERFACE

After the signal conditioning circuit has processed the real-time ECG signal, the user interface (UI) made with VP.in (Visual Programming Interface) is essential for viewing the signal. The user interface offers an interactive and dynamic representation of the ECG waveform once the raw ECG data is gathered from the manufactured electrode and conditioned via amplification and filtering. Both people and medical professionals can rapidly

distinguish between normal and abnormal cardiac rhythms because to the VP.in interface's visual representation of the data. The VP.in (Visual Programming Interface) enhances real-time ECG signal visualization, allowing users to monitor heart activity instantly. Its user-friendly design enables both medical professionals and general users to interpret ECG waveforms with ease. The interface supports automated signal analysis, detecting abnormalities and generating alerts for irregular heart rhythms. The peak detection in ECG signals is crucial for monitoring heartrate, identifying arrhythmias, diagnosing conditions, and supporting real-time patient monitoring in wearable devices. The user interface is used to find the R peak in the filtered ECG signal. The developed user interface and the respective code has been embedded in Arduino uno is shown in the Figure 12 and Figure 13.

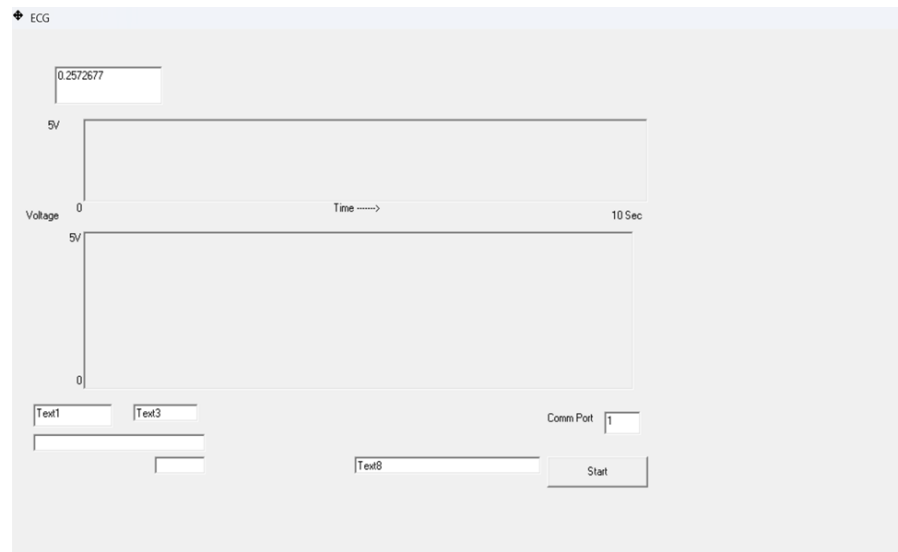


Figure 12: User Interface

```
void setup() {
  // set up the LCD's number of columns and rows:
  Serial.begin(115200);
  lcd.begin(16, 2);
  // Print a message to the LCD.
  pinMode(2, OUTPUT);
  pinMode(3, OUTPUT);
  pinMode(4, OUTPUT);
  pinMode(5, OUTPUT);
  digitalWrite(2, 0);
  digitalWrite(3, 0);
  digitalWrite(4, 0);
  digitalWrite(5, 0);
}
int hb,hbt,hbtt,cc,hc;
void loop() {
  // set the cursor to column 0, line 1
  // (note: line 1 is the second row, since counting begins with 0):
  // print the number of seconds since reset:
  sensorValue4 = 512-(analogRead(A0)/2);
  Serial.print("A");
  Serial.write((sensorValue4/100)+0x30);
  Serial.write(((sensorValue4%100)/10)+0x30);
  Serial.write((sensorValue4%10)+0x30);
  Serial.print("B");
}
```

Figure 13:Code embedded in the user interface



V. WORKING METHODOLOGY

The working methodology involves multiple stages, including signal acquisition, conditioning, processing, and analysis. The ECG signal is captured using a wearable electrode embedded with ZnO (Zinc Oxide) and graphene-based nanosensors, which enhance sensitivity and ensure accurate detection of bioelectric signals. These nanomaterials improve conductivity, reduce noise, and enhance skin-electrode contact for more precise ECG signal acquisition. Once the nanosensor-based electrode captures the weak ECG signals, the signal conditioning circuit processes the data. This stage includes amplification, where an instrumentation amplifier boosts the small bio-potential signals, followed by filtration to remove noise and unwanted frequencies, such as power line interference (50/60 Hz) and motion artifacts. A high-pass filter eliminates DC components, while a low-pass filter removes high-frequency noise. A notch filter used to eliminate specific noise frequencies. The conditioned signal is then fed into an Arduino Uno, which acts as the processing unit. The Arduino's ADC (Analog-to-Digital Converter) converts the analog ECG signal into a digital format for analysis. A peak detection algorithm is implemented within the Arduino to analyze ECG waveforms, with a specific focus on detecting the R-peak in the QRS complex. The R-peak is crucial for determining the heart rate and diagnosing cardiac abnormalities. Finally, the processed ECG signal is displayed on a user interface. This interface allows real-time visualization of ECG waveforms, R-peak detection, and heart rate monitoring. The system provides a compact, portable, and efficient solution for continuous ECG monitoring, making it suitable for wearable healthcare applications. The circuit diagram, proposed model and ECG wave from fabricated sensor is shown in the Figure 14, Figure 15, Figure 16.

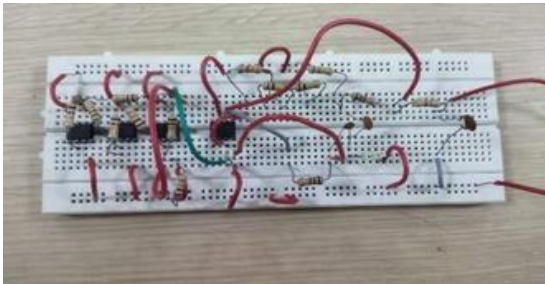


Figure 14 : Circuit diagram



Figure 15: Proposed model of the system

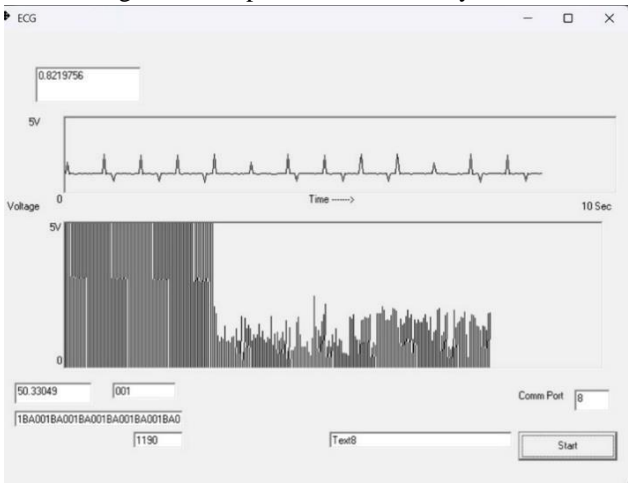


Figure 16:ECG wave from fabricated sensor



## VIII. RESULT AND DISCUSSION

The ECG signal acquisition and processing system's observation demonstrates how well the signal conditioning phases work to enhance the ECG waveform's quality. The instrumentation amplifier effectively amplifies the weak signals after obtaining the raw ECG signal from the body electrode. The notch filter eliminates power line interference, and the high-pass and low-pass filters remove high-frequency noise and low-frequency baseline wander. This produces a clear, uncluttered ECG signal that faithfully captures the electrical activity of the heart, which may then be examined for diagnostic purposes. The nanosensor-based ECG system demonstrates superior performance over conventional electrodes, as proven through key statistical metrics such as accuracy, noise reduction (NR), and signal-to-noise ratio (SNR). The accuracy of the nanosensor ECG system is calculated using the formula:

$$\text{Accuracy (\%)} = \left( \frac{\text{True positives} + \text{True negatives}}{\text{Total samples}} \right) \times 100$$

This results in 98.5% accuracy, compared to 92% for conventional electrodes, ensuring more reliable cardiac rhythm detection. Noise reduction (NR) is evaluated using formula:

$$\text{NR (dB)} = 10 \log_{10} \left( \frac{P_{\text{noise before}}}{P_{\text{noise after}}} \right),$$

This shows a 25 dB noise reduction for nanosensors, significantly better than the 10 dB achieved by conventional electrodes. This improved noise suppression leads to clearer ECG signals with reduced baseline drift and motion artifacts. Additionally, the signal-to-noise ratio (SNR), given by

$$\text{SNR (dB)} = 10 \log_{10} \left( \frac{P_{\text{signal}}}{P_{\text{noise}}} \right)$$

This confirms the nano sensor's superiority, with an SNR of 35 dB, compared to 20 dB for conventional electrodes. This means nanosensor ECG systems provide cleaner, more stable signals with minimal interference, improving diagnostic accuracy.

## IX. FUTURE ENHANCEMENT

The future scope will have advances in nanotechnology thus lead to smaller, more discreet sensors that users can wear comfortably. These Nano sensors will enhance data accuracy, providing more precise ECG readings. Integration with mobile devices will facilitate instant data analysis and feedback, making remote monitoring a viable option, especially in rural areas. This technology paves the way for personalized medicine, where data can inform tailored treatment plans based on individual health trends. Furthermore, AI and machine learning will analyze ECG data for predictive insights, identifying potential health risks before they manifest. Future devices may also incorporate multi-parameter monitoring, offering a comprehensive view of overall health. As regulatory frameworks evolve, innovative wearable devices will receive faster approvals, promoting widespread adoption. Ultimately, this technology could significantly improve population health management and early disease detection, transforming how we approach cardiac care.

## X. CONCLUSION

The implementation of Nano sensor in ECG signal monitoring demonstrates a significant advancement over conventional electrodes. The Nano sensor captures ECG signals with heightened sensitivity, enabling the detection of subtle bioelectric variations that traditional electrodes might overlook. Amplifying and filtering the Nano sensor signals using appropriate circuits ensures high signal quality and minimizes noise, enhancing the accuracy of heart condition analysis. Furthermore, the comparative analysis between signals from normal electrodes and Nano sensor highlights Nano sensor superior performance in terms of signal clarity and consistency. We collected the samples systematically, adhering to established guidelines to ensure reliable. The new nanosensor-based ECG system greatly improves accuracy, reduces noise, and makes signals clearer. However, to be used widely, we need to solve problems related to making it bigger, its cost of production, and its stability over time. Future efforts can concentrate on making inexpensive mass production and improving longevity with better biocompatible materials.

## REFERENCES

- [1] Gifari, M. W., Zakaria, H., & Mengko, R. (2015, August). Design of ECG Homecare: 12-lead ECG acquisition using single channel ECG device developed on AD8232 analog front end. In *2015 International Conference on Electrical Engineering and Informatics (ICEEI)* (pp. 371-376). IEEE.
- [2] Ahmad, M. A. (2016). Piezoelectric extraction of ECG signal. *Scientific Reports*, 6(1), 37093.
- [3] Faggion, L., & Mahdi, A. E. (2011, October). Noncontact human electrophysiological measurements using a new displacement current sensor. In *SENSORS, 2011 IEEE* (pp. 296-299). IEEE.
- [4] Hadizadeh, E., Rabbani, R., Azizi, Z., Barekatin, M., Hakhamaneshi, K., Khoram, E., & Fotowat-Ahmady, A. (2019). Ultra low-power system for remote ECG monitoring. *arXiv preprint arXiv:1903.08835*.
- [5] Yin, L., Chen, Y., & Ji, W. (2011, September). A novel method of diagnosing coronary heart disease by analysing ECG signals combined

with motion activity. In *2011 IEEE International Workshop on Machine Learning for Signal Processing* (pp. 1-5). IEEE.

[6] Biswas, U., & Maniruzzaman, M. (2014, April). Removing power line interference from ECG signal using adaptive filter and notch filter. In *2014 international conference on electrical engineering and information & communication technology* (pp. 1-4). IEEE.

[7] Bai, Y., He, S., & Wei, K. (2021, July). Design of a signal regulating circuit for wearable ECG sensor applications. In *2021 3rd International Conference on Intelligent Control, Measurement and Signal Processing and Intelligent Oil Field (ICMSP)* (pp. 173-176). IEEE.

[8] Datta, J., Saha, S., Chowdhury, S., & Acharya, A. (2017, March). Development of an ECG signal acquisition module. In *2017 Devices for Integrated Circuit (DevIC)* (pp. 419-421). IEEE.

[9] Purohit, S., Agrawal, Y., Gohel, B., Palaparthi, V., & Parekh, R. (2021, August). Capacitive Electrode Based Single Lead ECG Detection. In *2021 8th International Conference on Signal Processing and Integrated Networks (SPIN)* (pp. 903-908). IEEE.

[10] Almalchy, M. T., Ciobanu, V., & Popescu, N. (2019, May). Noise removal from ECG signal based on filtering techniques. In *2019 22nd International Conference on Control Systems and Computer Science (CSCS)* (pp. 176-181). IEEE.

[11] M. Tlili, A. Maalej, M. Ben Romdhane, F. Rivet, D. Dallet and C. Rebai, "Mathematical modeling of clean and noisy ECG signals in a level-crossing sampling context," *2016 International Symposium on Signal, Image, Video and Communications (ISIVC)*, Tunis, Tunisia, 2016, pp. 359-363, doi: 10.1109/ISIVC.2016.7894015.

[12] J. Ma, "Two-stage Amplifier Design for ECG Signal Processing," *2023 IEEE 6th International Conference on Information Systems and Computer Aided Education (ICISCAE)*, Dalian, China, 2023, pp. 794- 799, doi: 10.1109/ICISCAE59047.2023.10393791.

[13] L. Zhang and X. Jiang, "Acquisition and analysis system of the ECG signal based on LabVIEW," *2009 9th International Conference on Electronic Measurement & Instruments*, Beijing, China, 2009, pp. 4- 537-4-539, doi: 10.1109/ICEMI.2009.5274641.

[14] Y. Bai, S. He and K. Wei, "Design of a Signal Regulating Circuit for Wearable ECG Sensor Applications," *2021 3rd International Conference on Intelligent Control, Measurement and Signal Processing and Intelligent Oil Field (ICMSP)*, Xi'an, China, 2021, pp.173-176, doi: 10.1109/ICMSP53480.2021.9513370.

[15] S. Wang, X. Liu, X. Zhan and H. Liao, "Experimental characterization of detecting and processing method for ECG applications," *2015 IEEE International Conference on Electron Devices and Solid-State Circuits (EDSSC)*, Singapore, 2015, pp. 551-554, doi: 10.1109/EDSSC.2015.7285173.

[16] P. Siwindarto, A. B. Dianisma, Z. Abidin and S. S. Mahmudov, "ECG Signal Processing for Early Detection of Atrial and Ventricular Fibrillation Based on R-R Interval," *2020 10th Electrical Power, Electronics, Communications, Controls and Informatics Seminar (EECCIS)*, Malang, Indonesia, 2020, pp. 142-146, doi: 10.1109/EECCIS49483.2020.9263454.

[17] S. Thomas, J. S. Virdi, A. Verma, B. P. Das, K. Okada and P. N. Singh, "A Peak-detector-based Ultra Low Power ECG ASIC for Early Detection of Cardio-Vascular Diseases," *2024 IEEE International Symposium on Circuits and Systems (ISCAS)*, Singapore, Singapore, 2024, pp. 1-5, doi: 10.1109/ISCAS58744.2024.10558031